EXPERIMENT ON THE FORECAST OF CHARACTERISTIC QUANTITIES OF ATMOSPHERIC TURBULENCE BY MESOSCALE MODEL MM5*

ZHAO Ming (赵 鸣), *XU Liren* (许丽人) and *TANG Jianping* (汤剑平)

Key Laboratory for Mesoscale Severe Weather of Ministry of Education and Department of Atmospheric Sciences, Nanjing University, Nanjing 210093

Received January 8, 2001; revised July 10, 2001

ABSTRACT

In nested nonhydrostatic mesoscale model MM5, the characteristic quantities of atmospheric turbulence, i.e., the standard deviations of the turbulent fluctuated speeds for three directions in PBL are computed by Mellor-Yamada's level 2.5 closure scheme. The magnitudes and the vertical profiles of these quantities computed from the model are closely connected with temperature and wind speed profiles as well as the type of the ground with a significant diurnal variation, and are in agreement with known magnitudes and regularities in different stratification conditions. Hence the method in this paper is reasonable and convincible. Their horizontal distribution depends on the horizontal distribution of the stratification. The method of predicted characteristic quantities of turbulence from mesoscale model in this paper can be used in the problem of atmospheric diffusion and atmospheric environment.

Key words: atmospheric turbulence, standard deviation of turbulent speed, mesoscale model MM5, level 2.5 closure scheme

I. INTRODUCTION

As well known, understanding the structure of atmospheric turbulence is very important for understanding the atmospheric ability of diffusion as well as the prediction and control of air pollution. Usually the characteristic quantities of atmospheric turbulence, such as the variance and standard deviation of the turbulent fluctuated speed, are obtained from observations and some empirical laws are summarized. Kaimal et al. (1976), Panofsky et al. (1977) analyzed observed data and derived some empirical formulas. Caughey and Palmer (1979), Brost and Lenschow (1982), Grant (1986), De Bruin et al. (1993), Erbrink (1995) analyzed turbulence data in PBL (planetary boundary layer) respectively. Derbyshire (1995) analyzed the variance and covariance of the turbulent quantities in stable stratification. Founda et al. (1997) studied the standard deviation over complex terrain based on observations. Xu et al. (1997) studied the standard deviation of turbulent fluctuated speed in surface layer over Nanjing area. Lei et al. (1998) studied the characteristics of the turbulent quantities based on the observation in Chongqing area. Liu and Hong (2000) analyzed the data in Tibetan Plateau. Zhang and

* This work was supported by National Natural Science Foundation of China under Grant No. 49875005.

Zhao (1997) analyzed the standard deviation of turbulent speed over Gobi area in western China for different weather conditions. Stull (1988) summarized previous research works. All the above works obtained interesting results. In fact, the observation for turbulence is difficult and hence, not enough, especially in the boundary layer above surface layer. On the other hand, the simulation of the characteristic quantities of turbulence field by numerical model is an appropriate method. Wyngaard (1974a; 1974b; 1975) simulated the variance of the turbulent speed by using higher order closure. Derbyshire (1995) compared the observation with the large eddy simulation, Sullivan et al. (1994), Mason and Brown (1994) analyzed the variance of the turbulent speed by using the large eddy simulation method. Sharan and Gopalakrishnan (1999) studied the variation regularity of $\overline{w^2}$ with height for stable stratification. Andren (1990) diagnosed the turbulent quantities by using Mellor-Yamada's level 2.5 scheme in PBL model and compared to the observed data. Heilman and Takle (1991) diagnosed the turbulence characteristic quantities in PBL model by level 2.5 scheme. Hurley (1997) simulated the turbulence by use of mesoscale model, but only performed some experiments under ideal conditions. All the above numerical works did not use operational mesoscale model and realistic meteorological data, hence the routine prediction of these turbulence characteristic quantities can not be performed.

In this paper, we use nested nonhydrostatic mesoscale model MM5 incorporated with Mellor-Yamada's level 2.5 turbulence closure model to simulate the turbulence in a limited domain. The horizontal resolution for the large domain is 60 km which is appropriate for the sounding data in China, but 20 km for small (nested) domain, we then can simulate and predict the turbulence quantities at model grids for different times, which is useful for the application in the environment problem such as air pollution forecast etc. The simulated variances or standard deviations of the turbulent speed represent the mean values over a grid scale. The results show that the simulated characteristic quantities of turbulence are in agreement with known regularities, therefore, the scheme of this paper may provide a method to predict the characteristic quantities of turbulence from operational numerical model.

II. MODEL, DATA AND ANALYSIS METHOD

Nonhydrostatic MM5 model in a limited area is used in this paper, the governing equations include the forecast equations of wind speeds, temperature, pressure and humidity, the details may be found in Grell et al. (1994). 16 layers in σ coordinate system are selected, i.e., $\sigma=0.0, 0.1, 0.2, 0.3, 0.4, 0.5, 0.6, 0.7, 0.80, 0.85, 0.89, 0.93, 0.96, 0.98, 0.99$ and 1.0.

Grell's scheme for cumulus convection parameterization is chosen and Mellor-Yamada's level 2.5 scheme for PBL parameterization is used to compute the turbulent fluxes. For large domain, the grid numbers are $55\times65\times15$ and $40\times41\times15$ for case 1 and case 2 respectively, but for small domain, $34\times37\times15$ and $37\times40\times15$ are chosen for case 1 and case 2 respectively. The central points are (32°N, 107°E), (36°N, 117°E) for case 1 and case 2 respectively. Relaxation boundary condition is applied for large domain, but time-dependent and inflow-outflow conditions are used for small domain. The time step is 180 seconds.

NCEP reanalyzed data are used to run the model, the horizontal resolution of the data is 2.5°×2.5°, which are used to obtain initial field and lateral boundary condition. Case 1 is from 00 UTC 2 Jan. to 00 UTC 3 Jan. 1995. In the chart at 00 UTC 2 Jan., there was fine weather over large part of northern China due to the high pressure situation, but overcast or weak rainy weather over Changjiang-Huaihe Basins and southern China. Case 2 is from 00 UTC 22 Oct. to 00 UTC 23 Oct. 1994, the chart at 00 UTC 22 Oct. shows that fine weather controlled large part of China except small part in Southwest China, and maintained in the predicted 24 hours to follow.

The level 2.5 PBL parameterization scheme can not only compute the turbulent fluxes, but also predict turbulence kinetic energy. Then, after the kinetic energy is known, ten algebraic equations can be solved to find the variances or standard deviations of the turbulent speeds.

According to Mellor and Yamada (1982), for level 2.5 scheme, ten second-order moments of turbulence satisfy the following equations:

$$\overline{u^2} = \frac{q^2}{3} + \frac{l_1}{q}\left[-4\,\overline{wu}\,\frac{\partial U}{\partial z} + 2\,\overline{wv}\,\frac{\partial V}{\partial z} - 2\beta g\,\overline{w\theta}\right], \tag{1}$$

$$\overline{v^2} = \frac{q^2}{3} + \frac{l_1}{q}\left[2\,\overline{wu}\,\frac{\partial U}{\partial z} - 4\,\overline{wv}\,\frac{\partial V}{\partial z} - 2\beta g\,\overline{w\theta}\right], \tag{2}$$

$$\overline{w^2} = \frac{q^2}{3} + \frac{l_1}{q}\left[2\,\overline{wu}\,\frac{\partial U}{\partial z} + 2\,\overline{wv}\,\frac{\partial V}{\partial z} + 4\beta g\,\overline{w\theta}\right], \tag{3}$$

$$\overline{uv} = \frac{3l_1}{q}\left[-\overline{wu}\,\frac{\partial V}{\partial z} - \overline{wv}\,\frac{\partial U}{\partial z}\right], \tag{4}$$

$$\overline{wu} = \frac{3l_1}{q}\left[-(\overline{w^2} - C_1 q^2)\,\frac{\partial U}{\partial z} + \beta g\,\overline{u\theta}\right], \tag{5}$$

$$\overline{wv} = \frac{3l_1}{q}\left[-(\overline{w^2} - C_1 q^2)\,\frac{\partial V}{\partial z} + \beta g\,\overline{v\theta}\right], \tag{6}$$

$$\overline{u\theta} = \frac{3l_2}{q}\left[-\overline{wu}\,\frac{\partial \Theta}{\partial z} - \overline{w\theta}\,\frac{\partial U}{\partial z}\right], \tag{7}$$

$$\overline{v\theta} = \frac{3l_2}{q}\left[-\overline{wv}\,\frac{\partial \Theta}{\partial z} - \overline{w\theta}\,\frac{\partial V}{\partial z}\right], \tag{8}$$

$$\overline{w\theta} = \frac{3l_2}{q}\left[-\overline{w^2}\,\frac{\partial \Theta}{\partial z} + \beta g\,\overline{\theta^2}\right], \tag{9}$$

$$\overline{\theta^2} = -\frac{\Lambda_2}{q}\,\overline{w\theta}\,\frac{\partial \Theta}{\partial z}, \tag{10}$$

where $l_1=A_1 l$, $l_2=A_2 l$, $\Lambda_2=B_2 l$, A_1, A_2, B_2 and C_1 are equel to 0.92, 0.74, 10.1 and 0.08, respectively. l is mixing length (Mellor and Yamada 1982); U, V and Θ are variables predicted from mesoscale model; q^2 is the double of turbulent kinetic energy; and $\beta=g/T$.

There are 10 unknown variables in the 10 equations (1)—(10), we use elimination method to solve the equations, thus, we find the variances of turbulent speeds $\overline{u^2}$, $\overline{v^2}$, and $\overline{w^2}$. The obtained $\overline{u^2}$, $\overline{v^2}$ and $\overline{w^2}$ are the turbulent fluctuated speed variances along x, y, z directions in MM5 model. However, the variances or standard deviations in the wind direction coordinate system (taking x axis as wind direction) are more useful in atmospheric diffusion problem. We may find the variances in the wind direction coordinate system from the second-order moments in the MM5 coordinate system (see Appendix). The following variances or standard deviations in this paper are the values in the wind direction coordinate system.

III. RESULTS OF SIMULATION

We mainly analyze the nested small domain. Because there were no corresponding observed turbulence data for verification, we will see whether the simulated results obey the general law of the turbulence quantities. The model area for case 1 includes a large part of China, the southwest corner of the nested small domain is located at point (34,43) in large domain, the small domain includes part of North China and Bohai Sea. Figure 1 is the sea level pressure field in large domain for case 1. The northwesterly wind with fine weather predominated in the small domain. The model area for case 2 includes a large part of central and eastern China, the southwest corner of the nested small domain is located at point (16,16). The small domain also includes part of North China and Bohai Sea, there was northerly wind with fine weather. On the whole, the predicted synoptic situation coincides with the observation well.

1. *Simulated Profiles for Turbulence Quantities*

The observations in the whole boundary layer (Lei et al. 1998; Stull 1988; Sorbjan. 1986) and the numerical simulation of the atmospheric turbulence (Stull 1988; Hurley 1997; Andren 1991; Moeng 1986) show that generally, for unstable stratification during daytime, the standard deviations of turbulent speed increase with height from ground, sometimes only a slight change with height occurs at the middle of PBL because the turbulence is enhanced by work done by buoyancy, but the deviations decrease with height at the upper part of PBL due to the weak turbulence near the top of PBL. However, they

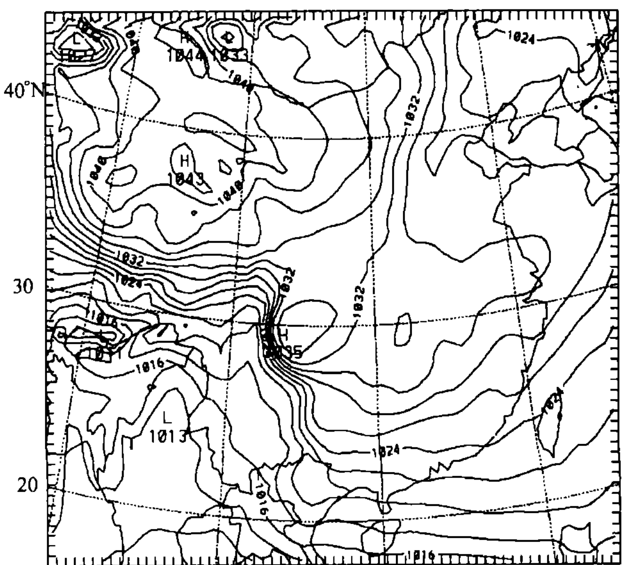

Fig. 1. The predicted 12 h sea level pressure field in large domain for case 1.

decrease with height for the stable stratification during night time due to the negative work done by the buoyancy and greater wind shear at lower part of PBL. The analysis for cases 1 and 2 shows that the profiles of the standard deviations of turbulent speed, wind and temperature are in agreement with the general regularities for almost all the grid points. The following is some examples.

Figure 2 is the simulated, $\sigma_{u,v,w}$, Θ and V profiles at point (4, 22) in nested small domain at 4th hour (1200 BT) for case 1, corresponding to the point (35, 50) in large domain. The simulated profiles are similar for these 2 points. It is seen from the potential temperature and wind profiles that there exists typical unstable stratification in PBL, the characteristics of the profiles for the standard deviations of the turbulent speed are in agreement with the above-mentioned general regularity, i. e., they increase with height at the lower part, then decrease with height at the upper part. The predicted PBL top height at 4th hour is 872. 2 m, which corresponds to the profile of turbulence very well. We also

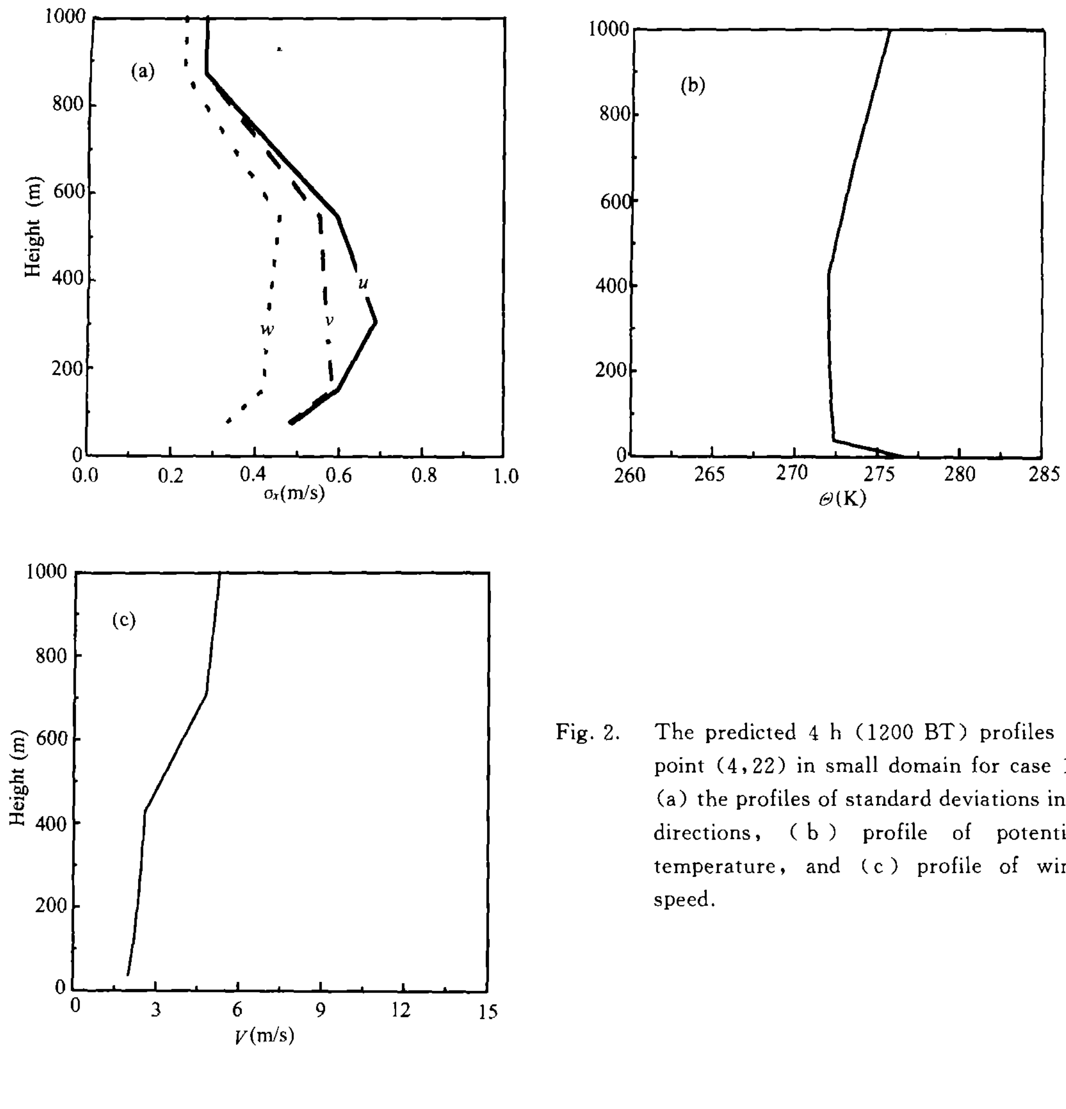

Fig. 2. The predicted 4 h (1200 BT) profiles at point (4, 22) in small domain for case 1: (a) the profiles of standard deviations in 3 directions, (b) profile of potential temperature, and (c) profile of wind speed.

can see $\sigma_u > \sigma_v > \sigma_w$. From the values of the standard deviation and the wind speed we can see that the turbulence intensities (the ratio of the standard deviations of turbulent speed to the wind speed) in 3 directions are about 0. 15 — 0. 25, a typical value for unstable condition. For example, EPA (1987) gave the lateral turbulence intensity about 0. 22 — 0. 3 and vertical turbulence intensity about 0. 14 — 0. 18 for the condition of class B of Pasquill's stability category (corresponding to typical unstable stratification) and wind speed lower than 4 m/s, and gave that the condition class E (corresponding to typical stable stratification) and wind speed less than 5 m/s corresponded to lateral turbulence intensity 0. 07 — 0. 13 and vertical turbulence intensity about 0. 04 — 0. 09, thus our magnitudes of the standard deviation are also reasonable. Figure 3 is the same profiles as in Fig. 2 at point (16,7) in small domain at 6th hour (1400 BT) for case 2, the profiles are similar to those at the corresponding points in large domain. All the profiles are also in agreement with the regularities for unstable conditions. The stratification is extremely unstable from the potential temperature and wind profiles (corresponding to class A) for this case, resulting in greater turbulence intensities.

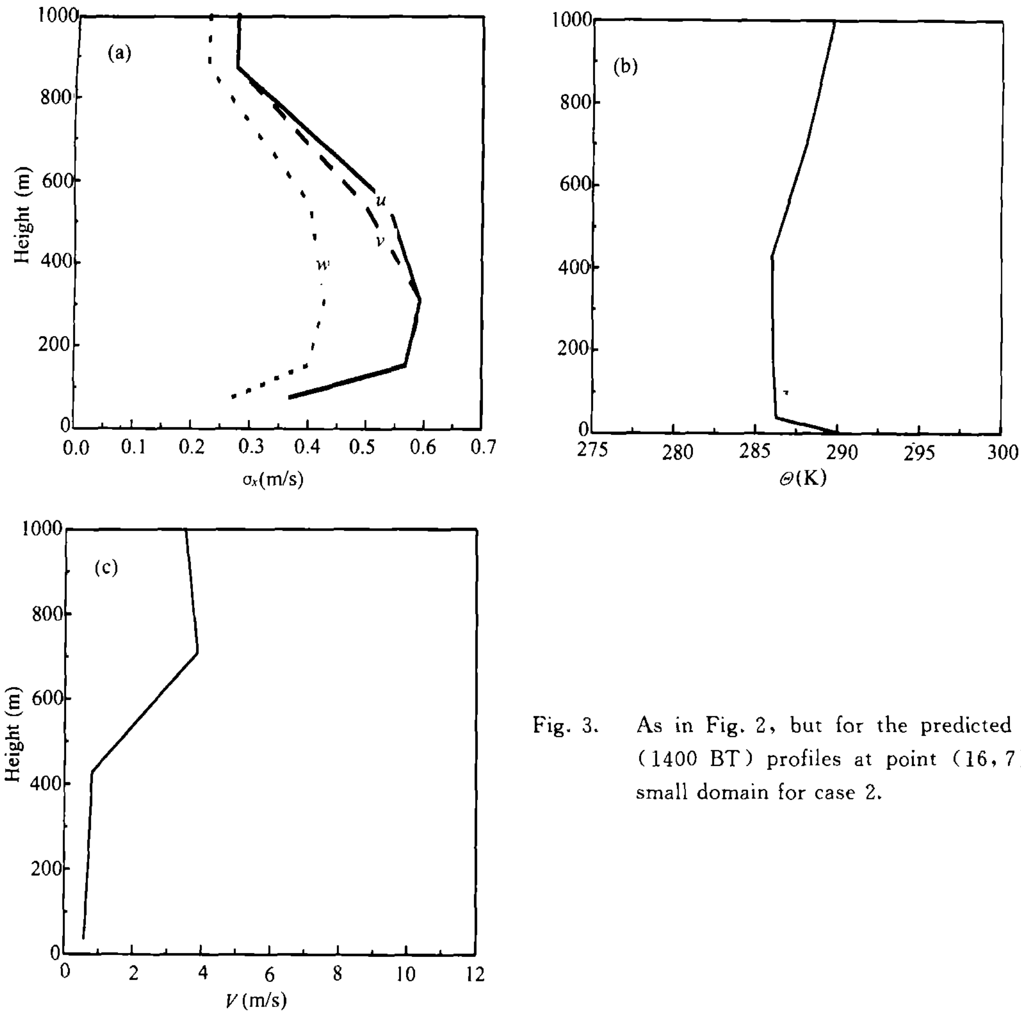

Fig. 3. As in Fig. 2, but for the predicted 6 h (1400 BT) profiles at point (16, 7) in small domain for case 2.

Figure 4 depicts the profiles of the standard deviations of turbulent speed, potential temperature and wind at point (25,20) in small domain at 19th hour (0300 BT) for case 1, the temperature and wind profiles show that the stratification is typical stable, the standard deviations in 3 directions all decrease with height. With a greater rate of decrease at lower part, then they almost do not change after the top of PBL is reached. All the profiles are in agreement with the regularity in stable conditions. The turbulence intensities in three directions at the lowest layer are 0. 11, 0. 07 and 0. 04, respectively, consistent with the values corresponding to above-mentioned class E.

The detailed analysis of the turbulence quantities in both large and small domains may obtain the following conclusions: The profiles of the standard deviations of turbulence speed in 3 directions, wind and potential temperature are connected closely with the stability, and obey the known general regularities for different stratifications. The profiles in large and small domains are similar. The profile for the standard deviations in small domain sometimes is more close to the general regularity. The analysis shows that the magnitudes of the standard deviations are also in agreement with the observed values.

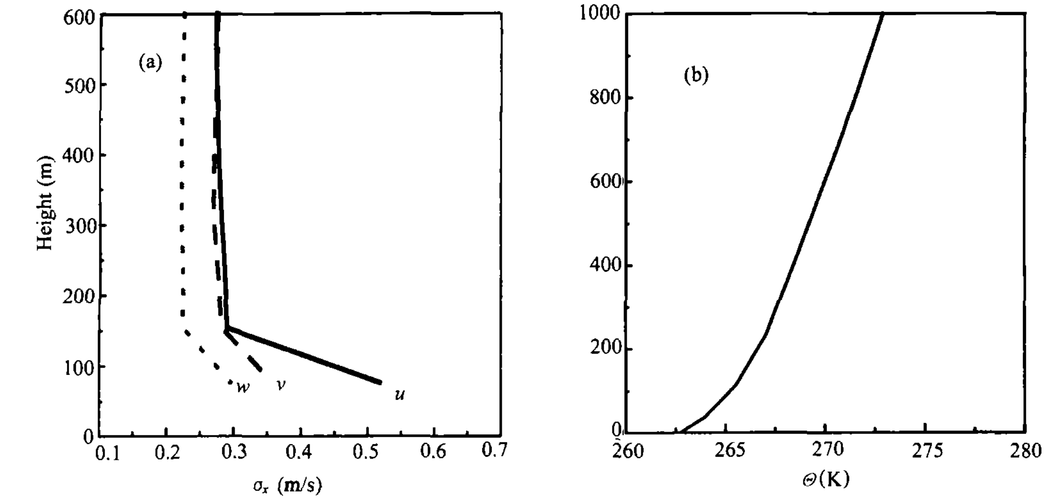

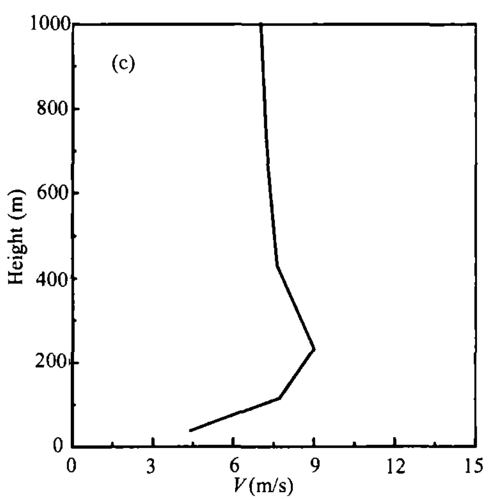

Fig. 4. As in Fig. 2 but for the predicted 19 h (0300 BT) profiles at point (25, 20) in small domain for case 1.

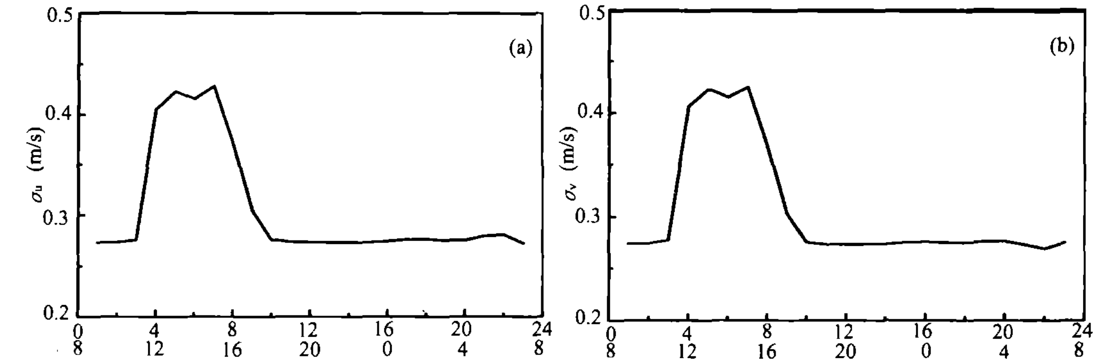

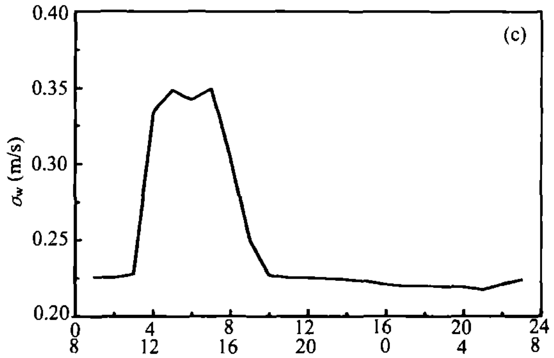

Fig. 5. The diurnal variation of the variances of the turbulence speed for 14th layer at point (19,19) in small domain for case 1. Charts (a), (b), and (c) are for u, v, and w directions respectively. The numbers on the first line of the abscissa represent the integral time of the model, the second line represents the corresponding Beijing Time.

2. *Simulated Diurnal Variations of Turbulence Quantities*

The analysis for different points shows that the 3 standard deviations of the turbulence speed all have significant diurnal variations, the following is some examples.

Figure 5 is the diurnal variation curves for the 3 standard deviations of turbulence speed (σ_u, σ_v and σ_w)on 14th level at point (19,19) whose ground is deciduous forest in small domain for case 1. It can be seen that all the 3 standard deviations increase with time after sunrise and attain maximum at noon or in afternoon, then decrease with time. The magnitude of σ_u is similar to or larger than σ_v, both are larger than σ_w. If we compare the standard deviations over different grounds in large domain, it may be found that the values over desert are greater than that over vegetation. This is because the stratification over desert is more unstable in daytime. The case 2 is similar to case 1.

3. *Horizontal Distributions of Turbulence Quantities*

The terrain in the nested small domain is flat relatively, we analyze the turbulence quantities on the σ surface, the following is the example for 15th layer.

Figure 6 is the terrain in the small domain for case 1, the terrain is higher near the west and north boundaries as well as in Liaodong and Shandong Peninsulas, other land surface is flat, the types of the ground surface are deciduous forest and sea. Figure 7 is the simulated vertical gradient of potential temperature at 15th layer in small domain. The

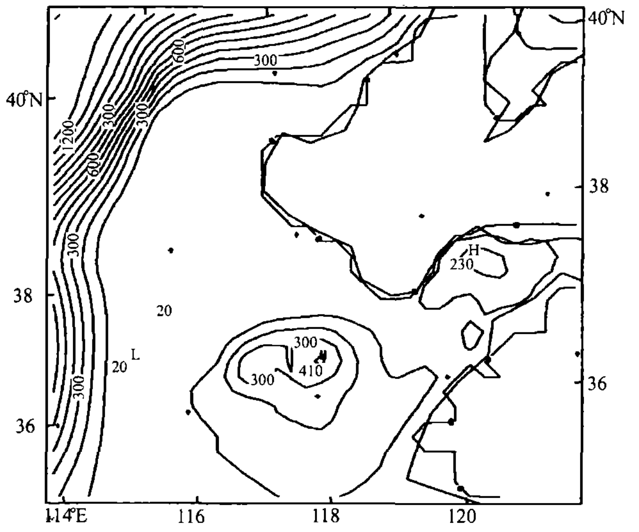

Fig. 6. The terrain in the nested small domain for case 1.

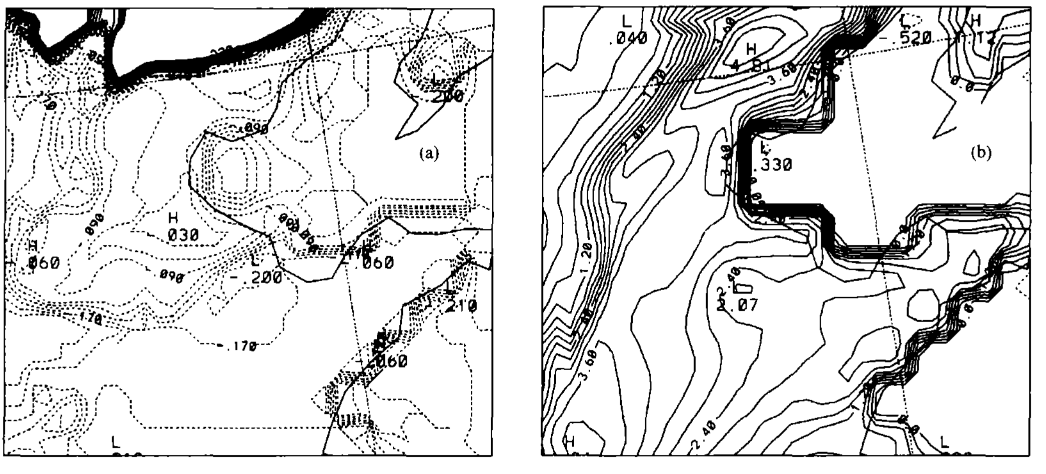

Fig. 7. The horizontal distribution of the vertical gradient of potential temperature at 15th layer in small domain for case 1. (a) The predicted vertical gradient of potential temperature at 4th hour (10^{-2}K/m); (b) the predicted vertical gredient of potential temperature at 16th hour.

predicted gradient at 4th hour (1200 BT) shows that the stratification is more unstable over land than that over sea, a concentrated distribution of contour appears near coastline; at 16th hour (0000 BT), the stratification over land is more stable than that over sea, there exists a similar concentrated distribution near coastline. Figure 8 is the horizontal distribution of the standard deviations of the turbulence speeds across wind direction at 15th layer in small domain, the figure shows that the standard deviations over land are greater than that over sea in daytime, there also exists a concentrated distribution near coastline. The greater horizontal gradient near coastline is due to the greater horizontal gradient of the vertical gradient of potential temperature near coastline. The standard

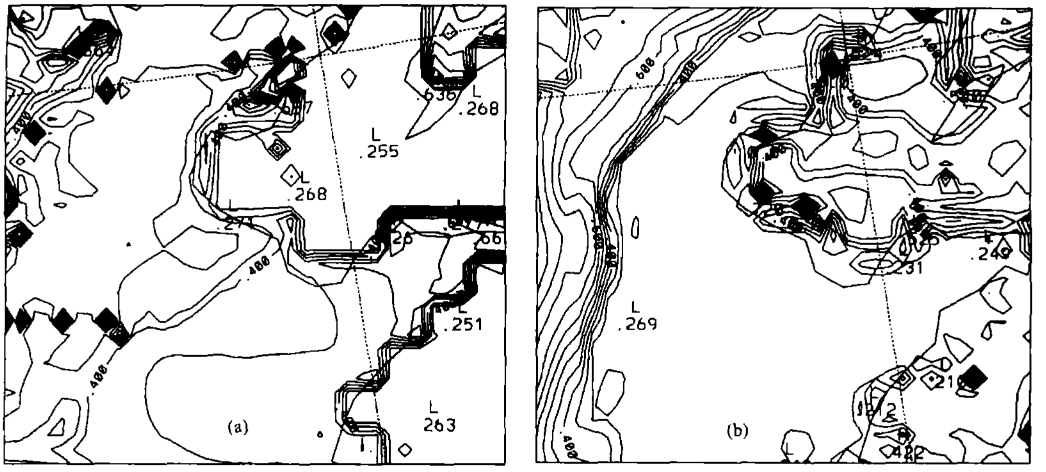

Fig. 8. The horizontal distribution of σ_v(m/s) at 15th layer in small domain for case 1: (a) the predicted values at 4th hour, and (b) the predicted values at 16th hour.

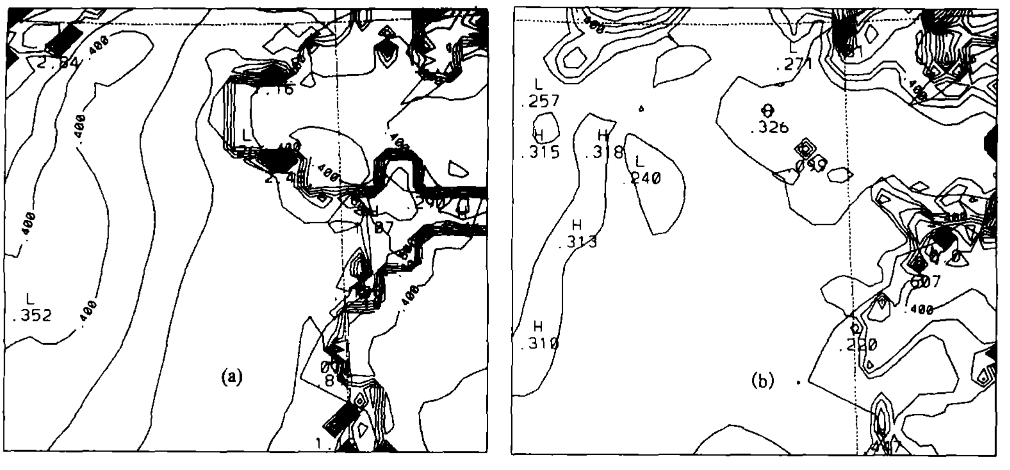

Fig. 9. The horizontal distribution of σ_u(m/s) at 15th layer in small domain for case 2: (a) the predicted values at 6th hour, and (b) the predicted values at 16th hour.

deviations are greater over the area at the northwest corner because of the higher terrain, which corresponds to the predicted vertical gradient of potential temperature at 4th hour very well. At 16th hour, the standard deviations are smaller over land than that over sea because the more stable stratification over land at night. We also find that the standard deviations are greater where the wind speed is stronger. The similar horizontal distribution appears for σ_u and σ_w. Figure 9 is the horizontal distribution of the standard deviations of the turbulence speed along wind direction at 15th layer for case 2, their characteristics of the horizontal distribution and the relation with the distribution of the vertical potential temperature gradient are similar to case 1, so are other 2 directions.

IV. SUMMARY

In this paper, the simplified second-order turbulence closure scheme level 2. 5 is incorporated in the nonhydrostatic MM5 model system, and used to simulate the turbulence for the cases 00 UTC 22 Dec. —00 UTC 23 Dec. , 1994 and 00 UTC 2 Jan. —00 UTC 3 Jan. , 1995. The simulation includes the temporal and spatial distributions for the standard deviations of the turbulence speed and the profiles of wind and potential temperature, we mainly research the temporal and spatial distributions of the standard deviations in the nested small domain, the following conclusions are summarized:

The standard deviations of the turbulence speed decrease with height in case of stable stratification with a greater rate of decrease in lower level; however, in case of unstable stratification, they increase with height in the lower part of PBL and decrease with height in the upper part, sometimes they change slightly in the middle of PBL, then decrease with height in the upper part until the top of PBL is reached. The standard deviations are also connected with the type of ground, the standard deviations over desert are larger than that over vegetation because the stratification is more unstable over desert during daytime. The standard deviations in 3 directions all display significant diurnal variation, they increase with time after sunrise, and attain maximum near noon, then decrease with time, attain minimum at night.

The 3 standard deviations all have a greater horizontal gradient near coastline both in daytime and nighttime because of the effect of temperature difference between sea and land. They connect closely with stratification, wind speed and terrain. The stratification is more unstable over land than that over sea in daytime, resulting in greater values of the standard deviation over land, the reverse is true at night. The greater values of the standard deviation occur where greater vertical gradient of potential temperature, greater wind speed and higher terrain exist.

From above summary, the level 2. 5 scheme incorporated with MM5 is useful and simple to predict the turbulence quantities and the results agree with known general regularity from observation and the numerical simulation of turbulence well, it can perform the simulation of the turbulence in the future time by the operational mesoscale model with less computer time, and provide the turbulence quantities in a limited area at a required time, further it can be used in air pollution forecast.

The vertical resolution of the model in this paper is not high enough, probably it can not catch some fine distributions, for example, at the lowest part of PBL, higher resolution probably can make more successful achievement.

APPENDIX: THE VARIANCES OF TURBULENCE SPEEDS IN WIND DIRECTION COORDINATE SYSTEM

Assuming that $\overline{\boldsymbol{V}}$ is mean wind vector, $\boldsymbol{V}$ is wind vector, and $\boldsymbol{V}'$ is fluctuated wind vector. $\overline{u^2}$, $\overline{v^2}$ and $\overline{w^2}$ are the variances of turbulence speed along x, y, z directions respectively in mesoscale model. $\overline{u_x^2}$ is the variance of turbulence speed along wind direction, and $\overline{v_x^2}$ is the variance of turbulence speed across wind direction. The following gives the derivation of their relation:

$$V' = \sqrt{u^2 + v^2}, \qquad (A.1)$$

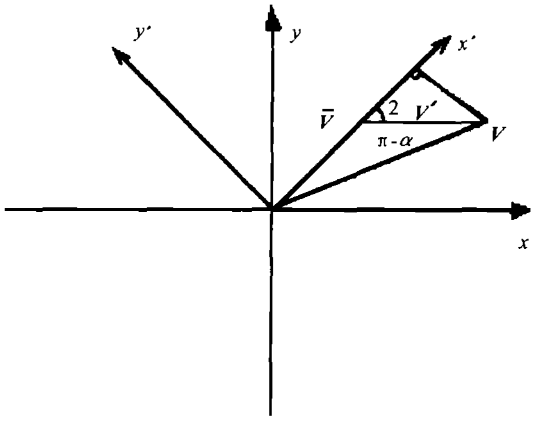

Fig. A1. Coordinate transformation, x', y' are the axes in the wind coordinate system.

$$u_x = V'\cos\alpha, \qquad v_x = V'\sin\alpha. \tag{A. 2}$$

According to the theorem in analytical geometry, we have

$$\cos\alpha = \frac{Uu + Vv}{\sqrt{U^2 + V^2}\sqrt{u^2 + v^2}}. \tag{A. 3}$$

Equation (A. 2) may be written as

$$\begin{cases} \overline{u_x^2} = \dfrac{U^2\,\overline{u^2} + 2UV\,\overline{uv} + V^2\,\overline{v^2}}{U^2 + V^2}, \\ \overline{v_x^2} = \dfrac{U^2\,\overline{v^2} - 2UV\,\overline{uv} + V^2\,\overline{u^2}}{U^2 + V^2}. \end{cases} \tag{A. 4}$$

Then we can find the variances in the wind direction coordinate system from the variances and second-order moment in the coordinate system in mesoscale model.

REFERENCES

Andren, A. (1990), Evaluation of a turbulence clousre scheme suitable for air pollution application, *J. Appl. Meteor.*, **29**: 224—239.

Andren, A. (1991), A TKE dissipation model for the atmospheric boundary layer, *Boundary Layer Meteor.*, **56**:207—221.

Brost, R. A. and Lenschow, H. (1982), Marine stratocumulus layer, Part II, Turbulence budget, *J. Atmos. Sci.*, **39**:818—836.

Caughey, S. J. and Palmer, S. G. (1979), Some aspects of turbulence structure through the depth the convective boundary layer, *Q. J. Roy. Meteor. Soc.*, **105**:811—827.

De Bruin H, A. R., Kohsiek, W. and Van Den Hurk, B. J. J. M. (1993), A verification of some methods to determining the fluxes of momentum, sensible heat, and water vapor using standard deviation and structure parameter of scalar meterorological quantities, *Boundary Layer Meteor.*, **63**: 231—257.

Derbyshire, S. H. (1995), Stable boundary layers observations, models and variability Part. I: Modeling and measurements, *Boundary Layer Meteor.*, **74**: 19—54.

EPA (USA) (1987), On-site meteorological program guideline for regulatory modeling applications, EPA —450/4—87—013, 172pp

Erbrink, J. J. (1995), Use of boundary layer meteorological parameters in the Gaussian model "Stacks", *Boundary. Layer Meteor.*, **74**: 211—235.

Founda, D., Tombrou, M., Lalas, D. P. and Asimakopoulos, D. N. (1997), Some measurements of turbulence characteristics over complex terrain, *Boundary Layer Meteor.*, **83**: 221—245.

Grant, A. L. M. (1986), Observations of the boundary layer structure made during the KONTUR experiment, *Q. J. Roy. Mete Soc.*, **112**:825—841.

Grell, G. A., Dudhia, J. and Stauffer, D. R. (1994), *A Description the Fifth-Generation Penn State/NCAR Mesoscale Model (MM5)*, NCAR Tech. Note NCAR/TN-398+STR.

Heilman, W. E. and Takle, E. S. (1991), Numerical simulation of the nocturnal turbulence characteristics over Rattlesnake mountain, *J. Appl. Meteor.*, **30**: 1106—1116.

Hurley, P. J. (1997), An evaluation of several turbulence schemes for the prediction of mean and turbulent fields in complex Terrain, *Boundary Layer Meteor.*, **83**:43—73.

Kaimal, J. C., Wyngaard, J. C., Haugen, D. A., Cote, O. R. and Izumi, Y. (1976), Turbulence structure in the convective boundary layer, *J. Atmos. Sci.*, **33**:2152—2169

Lei Xiaoen, Zhang Meigen and Han Zhiwei(1998), *The Basis and Model of Numerical Prediction on air Pollution*, China Meteor. Press, Beijing, 321pp. (in Chinese).

Liu Huizhi and Hong Zhongxiang (2000), The turbulence characteristics in the surface layer over Gaize area in Qinghai-Xizang Plateau, *Sinica Atmos. Sci.*, **24**:289—300 (in Chinese).

Mason, P. J. and Brown, A. R. (1994), The sensitivity of large-eddy simulations of turbulent shear flow to subgrid models, *Boundary Layer Meteor.*, **70**: 133—150.

Mellor, G. L. and Yamada, T. (1982), Development of a turbulence closure model for geophysical fluid problems, *Reviews of Geophysics and Space Physics*, **20**: 851—875.

Moeng, C-H. (1986), Large eddy simulation of a stratus-topped boundary layer, Part I, Structure and budget, *J. Atmos. Sci.*, **43**:2886—2900.

Panofsky, H. A., Tennekes, H., Lenschow, D. H. and Wyngaard, J. C. (1977), The characteristics of turbulent velocity components in the surface layer under convective conditions, *Boundary Layer Meteor.*, **11**: 355—361.

Sharan, M. and Gopalakrishnan, S. G. (1999), A local parameterization scheme for σ_w under stable conditions, *J. Appl. Meteor.*, **38**: 617—622.

Sorbjan, Z. (1986), On similarity in the atmospheric boundary layer, *Boundary Layer Meteor.*, **34**:377—397.

Stull, R. B. (1988), *An Introduction of Boundary Layer Meteorology*, Kluwer Academic Publishers, 666pp.

Sullivan, P. P., Mcwiliams, J. C. and Moeng, C-H. (1994), A subgrid-scale model for large-eddy simulation planetary boundary-layer flows, *Boundary Layer Meteor.*, **71**: 247—276.

Wyngaard, J. C. and Cote, O. R. (1974a), The evolution of a convective planetary boundary layer a higher order closure model, *Boundary Layer Meteor.*, **7**: 298—308.

Wyngaard, J. C., Cote, O. R. and Rao, K. S. (1974b), Modeling the atmospheric boundary layer, *Adv. Geophys.*, **18(A)**: 193—211.

Wyngaard, J. C. (1975), Modeling the planetary boundary layer, extension to the stable case. *Boundary Layer Meteor.*, **9**: 441—460.

Xu Yumao, Zhou Chaofu, Li Zongkai and Zhang Wei (1997), Turbulent structure and local similarity in the tower layer over the Nanjing area, *Boundary Layer Meteor.*, **82**: 1—21.

Zhang Qiang and Zhao Ming (1997), A preliminary analysis of the micrometeorological condition for different weather background over Gobi ground in Hexi area, *J. Nanjing University*, **33**:112—121 (in Chinese).